THE ASTROPHYSICAL JOURNAL, 392:264–271, 1992 June 10

THE HOPKINS ULTRAVIOLET TELESCOPE: PERFORMANCE AND CALIBRATION DURING THE ASTRO-1 MISSION

ARTHUR F. DAVIDSEN,[1] KNOX S. LONG,[1,2] SAMUEL T. DURRANCE,[1] WILLIAM P. BLAIR,[1] CHARLES W. BOWERS,[1] STEVEN J. CONARD,[1] PAUL D. FELDMAN,[1] HENRY C. FERGUSON,[3] GLEN H. FOUNTAIN,[4] RANDY A. KIMBLE,[5] GERARD A. KRISS,[1] H. WARREN MOOS,[1] AND KENNETH A. POTOCKI[4]

Submitted 1991 September 30; accepted 1991 December 19

ABSTRACT

The Hopkins Ultraviolet Telescope (HUT) was flown aboard the Space Shuttle *Columbia* on the Astro-1 mission 1990 December 2–11. Spectrophotometric observations of 77 astronomical sources were made throughout the far-ultraviolet (912–1850 Å) at a resolution of ~3 Å, and, for a small number of sources, in the extreme ultraviolet (415–912 Å) beyond the Lyman limit at a resolution of ~1.5 Å. The objects observed include quasars, galaxy clusters, active and normal galaxies, cataclysmic variables, globular clusters, supernova remnants, planetary nebulae, white dwarfs, Wolf-Rayet stars, Be stars, cool stars with active coronae, comet Levy (1990c), Jupiter, and Io. HUT has provided the first spectrophotometry in the sub-Lyman-α region for most of these sources. In this paper we describe the HUT instrument and its performance in orbit. We also present a HUT observation of the DA white dwarf G191-B2B and derive the photometric calibration curve for the instrument from a comparison of the observation with a model stellar atmosphere. The sensitivity reaches a maximum at 1050 Å, where 1 photon cm^{-2} s^{-1} $Å^{-1}$ yields 9.5 counts s^{-1} $Å^{-1}$, and remains within a factor 2 of this value from 912 to 1600 Å. The instrumental dark count measured on orbit was less than 10^{-3} counts s^{-1} $Å^{-1}$.

Subject headings: artificial satellites, space probes — instrumentation: spectrographs — stars: individual (G191-B2B) — ultraviolet: general — white dwarfs

1. INTRODUCTION

Ultraviolet astronomy has made enormous progress in the 14 years since the launch of the *International Ultraviolet Explorer* (*IUE*) (Boggess et al. 1978), and is poised for further advances as a result of the launch of the *Hubble Space Telescope*.[6] Both of these telescopes employ now-standard technology, including magnesium fluoride over-coated aluminum surfaces, which provide good reflectivity for wavelengths longer than ~1150 Å, and sealed-window detectors with magnesium fluoride or lithium fluoride windows, which provide transmission longward of 1150 and 1050 Å, respectively. Multiple reflections combine with the detector window transmission to limit these ultraviolet telescopes to a wavelength range which includes, at the short end, the Lyman-α line of hydrogen (1216 Å), but does not extend to the higher order lines in the Lyman series or the Lyman limit (912 Å).

The 912–1216 Å spectral region also contains the principal transitions of molecular hydrogen (the Lyman and Werner bands) and important transitions from commonly occurring ionization stages of other abundant elements, for example, O VI λλ1032, 1038. Furthermore, this wavelength region can provide a sensitive measure of the effective temperature of the hotter stars, for which the flux distribution longward of Lyman-α is a poor discriminator of T_e. Of course, observations shortward of the Lyman limit are also interesting, although for most sources the high opacity of interstellar hydrogen is expected to reduce drastically the observed flux just below 912 Å.

The astrophysically rich 912–1216 Å region has been explored previously in only fairly limited ways. *Copernicus* (Rogerson et al. 1973) obtained high-resolution spectra of the brightest stars in the 950–1450 Å range, primarily to study the interstellar medium (Spitzer & Jenkins 1975). The *Voyager* ultraviolet spectrometer (Broadfoot et al. 1977) has been employed to obtain low-resolution ($\Delta\lambda \geq 18$ Å) spectrophotometry of a number of sources from 500 to 1700 Å (Holberg 1990, 1991). Finally, several rocket-borne experiments have carried out a small number of observations in the far-ultraviolet (e.g., Brune, Mount, & Feldman 1979; Carruthers, Heckathorn, & Opal 1981; Woods, Feldman, & Bruner 1985; Cook, Cash, & Snow 1989).

The Hopkins Ultraviolet Telescope (HUT) was designed to perform moderate resolution ($\Delta\lambda = 3$ Å) spectrophotometry that would reach faint sources (e.g., quasars at $V \lesssim 16$) throughout the far-ultraviolet band from 830 to 1850 Å, with special emphasis on obtaining maximum performance in the 912–1216 Å band. In achieving this goal it was possible to make HUT sensitive to extreme ultraviolet (EUV) radiation as well, covering the range 415–925 Å in second order, without compromising or significantly complicating HUT's primary function. HUT was originally proposed to NASA in response to an Announcement of Opportunity for Spacelab missions aboard the Space Shuttle (Davidsen et al. 1978). An early description of the HUT design was given by Davidsen et al. (1981), and a more extensive discussion may be found in

[1] Department of Physics and Astronomy, The Johns Hopkins University, Charles & 34th Streets, Baltimore, MD 21218.
[2] Space Telescope Science Institute, 3700 San Martin Drive, Baltimore, MD 21218.
[3] Institute of Astronomy, University of Cambridge, The Observatories, Madingley Road, Cambridge, CB3 0HA, England.
[4] The Johns Hopkins University Applied Physics Laboratory, Johns Hopkins Road, Laurel, MD 20723-6099.
[5] Laboratory for Astronomy and Solar Physics, Code 681, NASA Goddard Space Flight Center, Greenbelt, MD 20771.
[6] The first imaging results may be found in a series of articles in ApJ, 369, L21–L78; the first spectroscopy is reported in ApJ, 377, L1–L64.

Davidsen & Fountain (1985). A detailed exposition of HUT's EUV capabilities is given by Davidsen et al. (1991a).

HUT was launched aboard the Space Shuttle *Columbia* as a component of the Astro-1 mission on 1990 December 2. It performed nearly flawlessly throughout the 9 day mission, obtaining almost 40 hours of observing time on 77 different sources. The first result from HUT, a limit on the lifetime of the τ neutrino in the decaying dark matter hypothesis of Sciama (1990, 1991), has been presented by Davidsen et al. (1991b). Other early results from HUT are presented in papers by Blair et al. (1991), Feldman et al. (1991), Ferguson et al. (1991), Kriss et al. (1992), Long et al. (1991), and Moos et al. (1991). In this paper we describe the HUT instrument and give a brief account of its performance and calibration during the Astro-1 mission.

2. INSTRUMENTATION

A schematic drawing of the HUT instrument is shown in Figure 1. The optical system consists of a 90 cm diameter *f*/2 primary mirror and a prime-focus, near-normal-incidence, Rowland-circle spectrograph. These elements are held in position by a rigid metering structure of low-expansion Invar. The entire assembly is housed within an aluminum environmental control canister, which protects against contamination on the ground and provides a thermally controlled, optically shielded environment during observations. The parabolic primary mirror is fabricated of Zerodur and figured to provide 1″ image quality at the focal plane. It is coated with iridium, which provides ~20% reflectivity in the primary 912–1216 Å range (and in the 500–600 Å range as well) and is stable in the low-Earth orbital environment. Three motorized mechanisms in the Invar mirror-mounting structure provide the capability to focus and align the instrument during the mission.

The prime focus spectrograph is housed in an evacuated stainless steel enclosure, whose vacuum is maintained at $\sim 10^{-6}$ torr by redundant Vac-Ion pumps. The spectrograph contains a 20 cm diameter f/2 spherical concave grating that was holographically generated (600 lines mm^{-1}) and overcoated with osmium. The depth of the sinusoidal groove profile is chosen to provide optimal first-order efficiency at ~1000 Å. Light passing through the spectrograph entrance aperture is diffracted and focused onto a photon-counting CsI-coated microchannel-plate intensifier at a dispersion of 41 Å mm^{-1}. The intensifier employs a chevron pair of 80:1 microchannel plates (MCPs) with 10 μm diameter pores and 25 mm active area, operated at a gain of 2×10^6. Charge pulses from the MCPs impinge on a P20 phosphor, whose visible light output is coupled via fiber optics to a one-dimensional 1024 element self-scanned photodiode array (Reticon) clocked at 1 scan ms^{-1}. A typical charge pulse covers ~8 photodiodes (200 μm) at threshold. Each pulse is centroided by an onboard computer, yielding a pixel size of 12.5 μm (half the diode width or 0.51 Å in first order), and is accumulated in a 2048 element spectral aray. The detector resolution is ~1 Å, but the aberrations of the f/2 optical system limit the effective resolution for a point source to about 3 Å in first order. The plate scale at the detector is 2.″8 $Å^{-1}$, so when the pointing is stable ($\pm 1''$) the resolution is not significantly degraded by image motion. The design and performance of an early version of the HUT detector have been described in more detail by Long et al. (1985).

To enable the instrument to be operated on the ground, a small mercury calibration lamp was included in the spectrograph. This lamp provides a line at 1849 Å that is imaged onto the detector by the grating. Monitoring this source at various stages throughout the shuttle integration confirmed the operation of the entire system, while the observed count rate provided a record of the sensitivity of the spectrograph at one wavelength over time.

An eight position rotating mechanism at the spectrograph entrance provides a choice among six aperture sizes and/or filters for observations, as well as two positions for ground operations (a vacuum seal position and a large aperture for calibration). Point-source observations are generally made through one of two circular apertures of 18″ and 30″ diameters. Extended source observations are generally made through one of two long-slit apertures with dimensions of 9.″4 × 116″ and 17″ × 116″, providing resolution of 3.3 and 6 Å, respectively. One of the observing positions contains a thin aluminum filter behind a 30″ diameter aperture, which strongly rejects the first-order FUV light and provides a pure EUV bandpass (415–700 Å). Finally, one position contains a 17″ × 116″ aperture and a CaF_2 filter, which provides the capability to exclude Lyman-α (and all wavelengths shorter than ~1250 Å) from the spectrograph.

The apertures were etched into a mirrored surface that reflects visible light from the surrounding star field through a re-imaging lens system and filter wheel onto the focal plane of a silicon intensified target (SIT) vidicon camera. The camera views a 9′ × 12′ field surrounding the spectrograph aperture with 2″ resolution. Digitized video images are analyzed by the onboard processor and compared with predefined target and guide star positions. Final target identification is made onboard by the payload specialist (an astronomer/astronaut chosen from the Astro instrument teams), who completes the acquisition by adjusting the instrument pointing system (IPS) on which HUT and the other Astro UV telescopes are mounted. Commandable adjustments to the camera gain and integration time, as well as selection of an appropriate neutral density filter wheel position, permit acquisition of targets with visual magnitudes ranging from −4 to +17.

HUT incorporates two custom-built microprocessors (Ballard 1984) that execute commands directly from the high-level language FORTH. The spectrometer processor (SP) handles the high-rate data from the Reticon, applying commandable pulse width and amplitude limits to the digitized Reticon output for noise rejection, calculating centroids of pulses, and creating telemetry messages in several possible formats. Of these output modes, two are principally used for the science data. The high-time-resolution mode provides a time-tagged list of each individual photon event, with an accuracy of ± 1 ms. This mode can be employed for sources whose total count rates do not exceed ~600 counts s^{-1}. For higher rate sources, histogram mode is employed, in which a cumulative 2048 element histogram is output to the telemetry every 2 s. This cumulative histogram is also downlinked every 60 s in high-time-resolution mode. Thus when data dropouts occur, only the photon arrival time information is lost, and the spectral data are preserved. The dedicated experiment processor (DEP) performs all the functions of command and control of the HUT instrument, and also digitizes, stores, and analyzes the video images from the target acquisition camera. The DEP also provides communications with the crew and with the science team at the Payload Operations Control Center in Huntsville, Alabama, via the Spacelab Experiment Computer on the Shuttle.

The HUT detector is limited by phosphor persistence, pulse size, and scan rate to total count rates $\lesssim$5000 counts s^{-1}. To observe targets with higher count rates, principally the

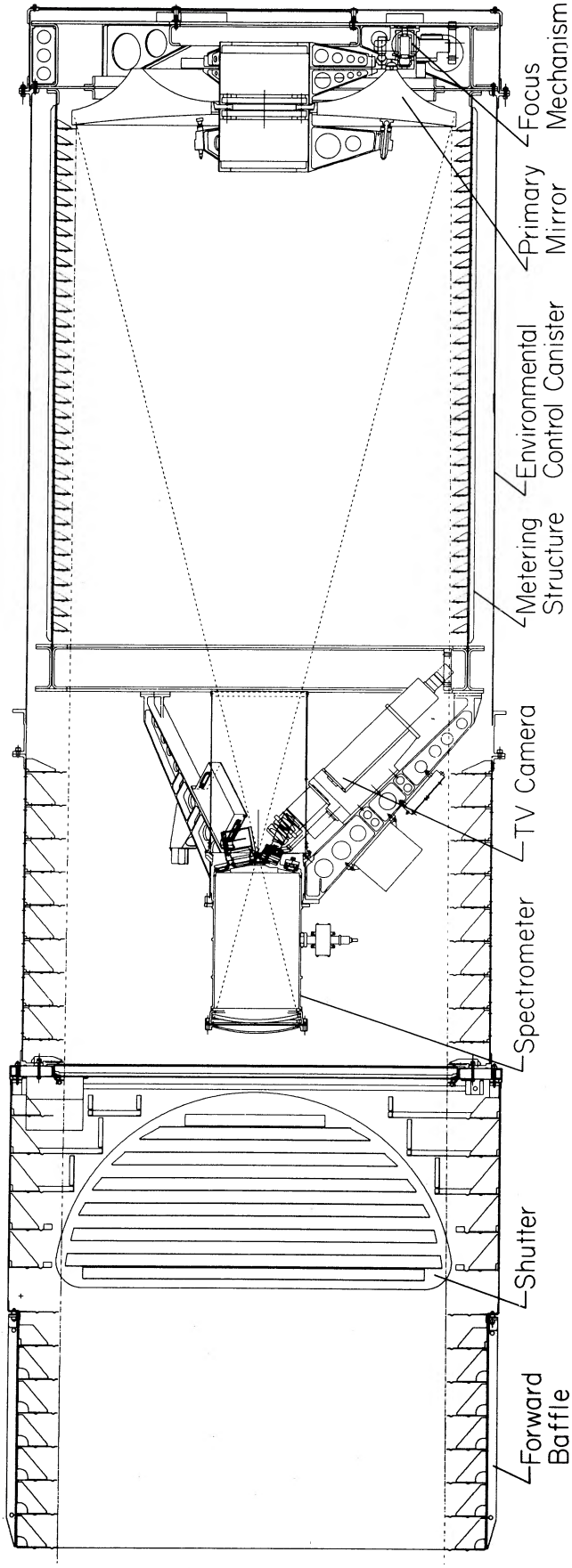

FIG. 1.—Drawing of the Hopkins Ultraviolet Telescope (plan view). Overall dimensions are 3.8 m × 1.1 m (diameter). Many of the principal components are labeled. Power supplies, computers, etc., are located in a separate electronics module, not shown.

brightest O and B stars, the HUT telescope aperture may be reduced from the nominal full aperture size of 5120 cm^2. A 50% reduction is accomplished by closing one of two semicircular shutter doors. Further reduction to 1% (50 cm^2) and 0.02% (1 cm^2) of full aperture can be made by closing both shutter doors and opening either of two small apertures provided for this purpose. In these apertures the spectrograph aberrations become negligible and the resolution improves to a detector-limited value of $\sim$1 Å (for stable pointing). The smallest aperture was not employed during the Astro-1 mission.

3. PERFORMANCE

The Astro-1 Observatory including the Hopkins Ultraviolet Telescope, was launched from Pad 39B at Kennedy Space Center aboard the Space Shuttle *Columbia* (STS-35) at 01:49 A.M. EST on 1990 December 2. The orbit achieved was nearly circular at an altitude of 358 km and an inclination of 28°.5. HUT's initial activation was performed as scheduled at 04:30 hours Mission Elapsed Time (MET), but first light, planned for 18:00 hours MET, was substantially delayed by several Spacelab system problems, including the failure of one of the two terminals used by the crew to command the experiments and the failure of the IPS to acquire targets. HUT obtained first light, observation of the airglow spectrum in the general direction of the Vela supernova remnant, at about 32 hours MET and observed the first source (the Seyfert galaxy NGC 4151) at 35 hours MET. Earlier planned observations intended to focus HUT and check its co-alignment with the other Astro instruments were not accomplished due to the problems mentioned above, but the first several successful observations persuaded us that HUT was adequately focused and aligned to proceed with observations.

Observations continued at least partially successfully until 101 hours MET, when the second terminal used by the crew also failed. A new operational mode was then developed, in which the instruments were commanded from the ground while the crew employed the manual pointing controller (similar to a guide paddle on a ground-based telescope) to acquire and guide on the targets. Successful operation in the new mode resumed at 118.5 hours MET and continued without any major difficulty until the final observation was made with HUT at 200 hours. This occurred one day earlier than planned due to concerns about the weather at the Shuttle landing site. Landing was at 215 hours MET at Edwards Air Force Base, California, and the payload was recovered in good condition.

During the Astro-1 mission, HUT obtained a total of 106 separate observations of 77 different sources, accumulating 39.4 hours of on-source integration time. Observations were made throughout each orbit and include varying contributions from the emission lines originating in Earth's atmosphere, the airglow. As expected, observations of the fainter sources and those requiring the larger apertures were best obtained while the orbiter was in Earth's shadow and the airglow lines were weaker, but the brighter point-source observations made effective use of the Sun-lit portion of the orbit. Among the objects observed successfully were quasars, galaxy clusters, active and normal galaxies cataclysmic variables, globular clusters, supernova remnants, planetary nebulae, white dwarfs, Wolf-Rayet stars, Be stars, cool stars with active coronae, comet Levy (1990c), Jupiter and Io.

Detector dark count was measured 3 times during the mission with the spectrograph aperture in the closed position. The rates obtained over the whole spectrum varied from 0.73 to 0.96 counts s^{-1}, with a mean of 0.80 $\pm$ 0.02 (mean error), corresponding to 7.7 $\times$ 10^{-4} counts s^{-1} Å^{-1}. This is approximately twice the rate observed during laboratory calibration, consistent with the more intense radiation environment encountered in orbit. A typical exposure with HUT ($\lesssim$2000 s) contains $\lesssim$1 dark count pixel^{-1}. No observations were made during passage through the South Atlantic Anomaly.

The dominant source of background in HUT observations is due to emission from Earth's geocorona, which was at a high level due to strong solar activity and a hot atmosphere at the time of the mission. The strongest line by far is H I Lyman-α, whose intensity was typically $\sim$3 kR (1 kR = $10^9/4\pi$ photons cm^{-2} s^{-1} sr^{-1}) at orbital midnight, yielding $\sim$12 counts s^{-1} in the smallest aperture (18″) and $\sim$100 counts s^{-1} in the largest aperture (17″ $\times$ 116″). During orbital day these rates were typically larger by a factor of 10. Other geocoronal lines observed at night include O I λ1304 and λ1356, Lyman-β, and He I λ584 in second and third orders. During orbital day, a multitude of additional lines appears below 1200 Å, mainly due to O I, N I, and N II. The FWHM of the airglow lines as measured with the narrow slit (9″) ranges from 3.2 to 3.5 Å, verifying the expected resolution of the spectrograph. The positions of the airglow lines were also used to determine the wavelength calibration in flight, which was found to be in good agreement with our laboratory calibrations. HUT wavelengths appear to be accurate to $\pm$0.5 Å in most cases. Most of this error results from uncertainties in the position of a source in the aperture.

Light scattered by the HUT diffraction grating is another source of background. Unlike the airglow lines, which are localized in wavelength, the scattered light component produces a continuum background. Preflight measurements of the holographic grating, selected for its low scattered light, gave a scattered continuum 50 Å away from a line of intensity I counts s^{-1} of $\lesssim 10^{-5}$ I counts s^{-1} Å^{-1}. We verified the low scattered light in HUT during the flight by measuring the apparent flux below 912 Å for each source. Except for the few EUV sources observed, this flux gives a direct measure of the sum of the dark counts and the scattered light. These measurements verified that both of these contributions to the background are very small and consistent with preflight expectations.

An example of the data obtained by HUT on the Astro-1 mission is shown in Figure 2, which gives the observed (raw) count spectrum for the DA white dwarf G191-B2B (V = 11.78). This observation was obtained through the 30″ point-source aperture with HUT stopped down to the half-aperture door position. It began at 03:19:31 GMT on 1990 December 5 and lasted for 366 s, during which the mean count rate was 2627 counts s^{-1}. The star was held within the spectrograph aperture throughout the observation, as indicated both by the constancy of the observed count rate and by the guide star position data. This object was also observed through the EUV filter aperture, and significant flux was measured at $\sim$500 Å (Kimble et al. 1992). The EUV observation allows us to infer that second- and third-order EUV radiation contributes a few percent of the peak counts observed in Figure 2, and it is straightforward to corect the observed spectum to obtain a pure first-order spectrum.

The only strong features in the G191-B2B spectrum are the Lyman absorption lines, as expected for an object believed to have a nearly pure hydrogen atmosphere. Lyman-α is partially

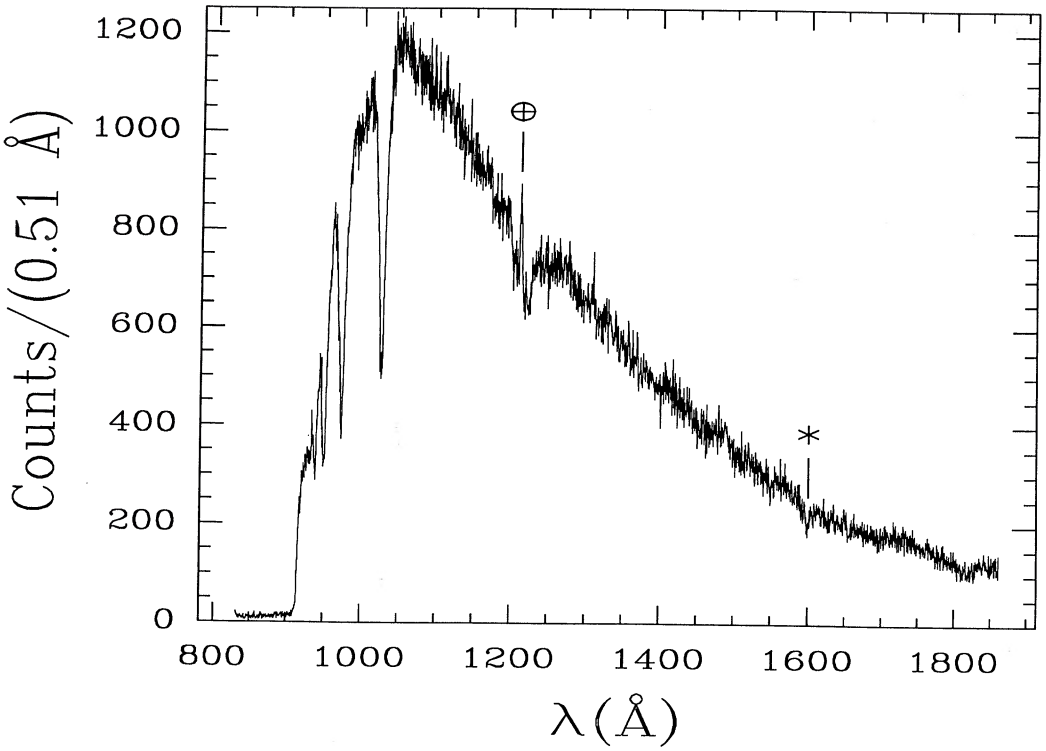

FIG. 2.—Observed (raw) count spectrum for a 366 s observation of the DA white dwarf G191-B2B. Pixels, 0.51 Å wide, have been converted to a wavelength scale. The Lyman-series lines are seen clearly. Lyman-α is partially filled in by geocoronal emission. The Lyman edge produced by interstellar hydrogen is also evident. The apparent absorption feature at 1600 Å, marked with an asterisk, is an artifact, due to a small dead spot on the detector.

filled in by the strong geocoronal emission at this wavelength, but the higher Lyman-series lines are much less affected. The continuum cuts off sharply below 915 Å, due to absorption by interstellar hydrogen in the converging Lyman series and the Lyman continuum. The small residual flux observed below 912 Å is due to second- and third-order radiation from ~450 and ~300 Å (~$\frac{2}{3}$ of the observed signal) and scattered light from $\lambda > 912$ Å (~$\frac{1}{3}$ of the signal). The apparent rise in the continuum longward of 1825 Å is due to a second-order contribution from $\lambda \gtrsim 912$ Å, which is easily corrected in reduced data. Finally, there is a weak apparent absorption feature at 1600 Å that we have determined to be due to a small dead region in the detector. This feature is not readily apparent in full-aperture observations, while it is very obvious in the 50 cm^2 aperture observations. The increased strength of the feature results from the much smaller astignatism in the small-aperture observations.

This observation of G191-B2B has been used to obtain the primary in-flight throughput calibration of HUT; a more detailed description of the HUT calibration will be presented in a future publication. Briefly, however, the observed spectrum was corrected for second- and third-order contributions, dark counts, phosphor persistence (which causes 7.4% of real events to be double-counted), and dead-time effects (~5% at the peak of this spectrum). The resulting spectrum was then compared with a model-atmosphere calculation for G191-B2B ($T_{\rm eff}$ = 59,250 K, log g = 7.5, and V = 11.78), described by Holberg et al. (1991) and kindly provided to us by P. Bergeron. Division of the corrected spectrum by the Bergeron model prediction, which has been multiplied by the transmission of the interstellar medium for $N_{\rm H} = 1.7 \times 10^{18}$ cm^{-2} and b = 10 km s^{-1} (Kimble et al. 1992) and then smoothed to the HUT resolution, yields the effective-area curve shown in Figure 3. The data in Figure 3 have also been multiplied by the ratio of full-aperture to half-aperture sensitivity, derived separately from observations of several stars that were observed in both the half-aperture and full-aperture modes.

The data in Figure 3 have been used to derive the HUT effective area curve (shown as the smooth curve). Structure on scales less than ~25 Å was removed by smoothing the raw data with a Gaussian of dispersion 10 Å. Before smoothing, 5 Å regions surrounding the cores of Lyβ, Lyγ, Lyδ, and the 1600 Å feature were replaced by linear interpolation of the surrounding pixels. A 15 Å region centered on Lyα was similarly replaced. Also shown in Figure 3 are effective areas at several wavelengths as computed from the efficiencies of various components of HUT measured in the laboratory several years before the mission. A full end-to-end laboratory calibration of the assembled instrument was not possible within the scope of the HUT program. The in-flight measurements run ~20%–30% below the preflight values, probably due to aging of the photocathode. Our measurements of the on-board calibration lamp over time indicate a decline in efficiency of 24%. We also measured a similar decline in sensitivity (in both magnitude and spectral shape) over several years in the original HUT spectrograph, which was replaced after the *Challenger* accident. The two low points in the preflight data, at 1280 and 1336 Å, were suspect, due to inadequate reference-detector calibrations at these wavelengths. To obtain the effective-area curve shortward of 920 Å, where the observed flux of G191-B2B goes to zero, we have used the preflight calibration points at 835, 879, and 920 Å. A linear least-squares fit was made to these points and scaled down (by 27%) to join smoothly onto the in-flight calibration curve at 920 Å. We consider the overall

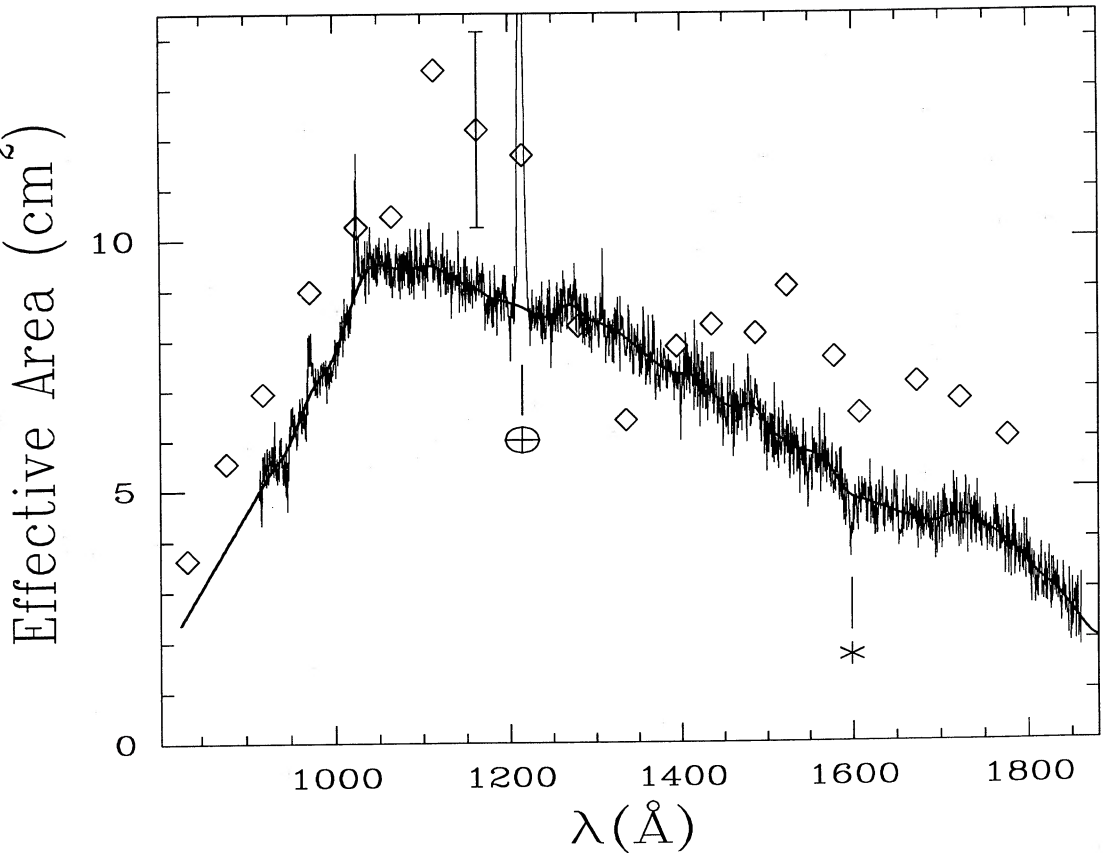

FIG. 3.—Effective area of HUT in first order, obtained by correcting the data of Fig. 2 for various effects (*see text*) and dividing by a model atmosphere for G191-B2B provided by P. Bergeron. The apparent emission features are at the wavelengths of Lyman-α, Lyman-β, and Lyman-γ. The smooth curve, used to generate flux-calibrated spectra from HUT data, was obtained by smoothing the data with a Gaussian, after eliminating the regions in the cores of the Lyman lines and near the detector artifact at 1600 Å (*see text*). The plotted points (*diamonds*) represent predicted values of the effective area based on preflight laboratory measurements of HUT components. A representative error bar is also shown. The two low points at 1280 and 1336 Å are suspect, due to inadequate cross-calibration of the laboratory reference detector (at these wavelengths only). The overall agreement is excellent, allowing for the long interval between the measurements, and the expected slow decay of the photocathode sensitivity.

agreement of the preflight and flight data to be highly satisfactory.

Figure 4 shows the adopted flux fit of G191-B2B to the Bergeron model. Also shown is an independent model calculation for the same $T_{\rm eff}$ and log g, kindly provided by D. Koester. Comparison of the data and the models gives some idea of the internal consistency of the calibration, although of course, it yields no information on possible systematic errors in absolute flux calibration. These could arise, for example, from deviations of the real white dwarf atmosphere from the model atmosphere or from unknown errors in our data reduction procedure. At present we believe that the calibration of the HUT sensitivity is accurate to better than ±10% throughout the 912–1800 Å band. Uncertainties in the G191-B2B temperature (derived from Balmer line profiles) translate to less than 5% changes in the model-predicted far UV flux down to within a few Å of the Lyman edge. Variations in the fitting procedure used to derive the effective area curve from the observation (judgements on how smooth the curve should be) lead to only ±5% excursions around the curve we have adopted. Therefore, since the statistical precision is also excellent, if the DA white dwarf model atmosphere is correct, the HUT sensitivity curve is extremely well determined.

Several lines of evidence support the belief that the G191-B2B model flux is accurate to the level cited. A comparison of the observed spectra for G191-B2B and the significantly cooler DA white dwarf HZ43 confirms the self-consistency of the model atmospheres employed. Independent of white dwarf models, a preliminary analysis of the HUT observation of the BL Lac object PKS 2155−304 indicates that, when fluxed with the G191-B2B–based calibration, the spectrum is well fitted by a power law all the way to the Lyman limit, as expected for this object. Finally, the ratio of the in-flight to preflight calibrations varies with wavelength by only 20%, and this is in a manner that is consistent with the degradation we have previously observed for detectors of this type. There is thus no reason to suspect any large calibration error of the magnitude that has plagued sub-Lyman-α spectrophotometric observations in the past (cf. Holberg et al. 1991 and references therein). Future papers will detail the comparisons of HUT data for other sources with model calculations and with *Voyager* and rocket data in order to develop further a reliable calibration for the far-ultraviolet region of the spectrum.

We have recently (1992 January) performed a postflight laboratory calibration of the HUT spectrograph at seven wavelengths distributed across our spectral range. The ratio of the postflight laboratory efficiencies is well fitted by a smooth curve varying from ∼0.85 to ∼0.65 across our first-order wavelength range. This degradation is consistent with our previous experience as described above. The preflight effective

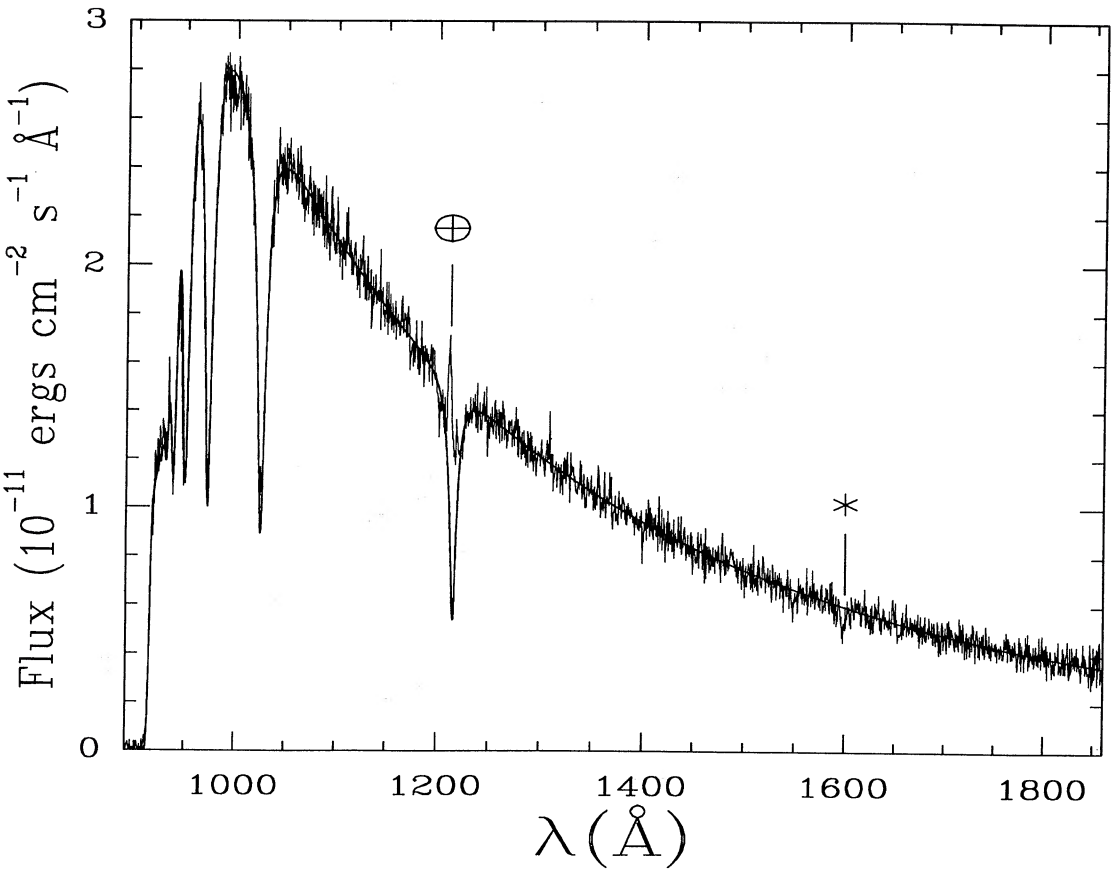

FIG. 4a

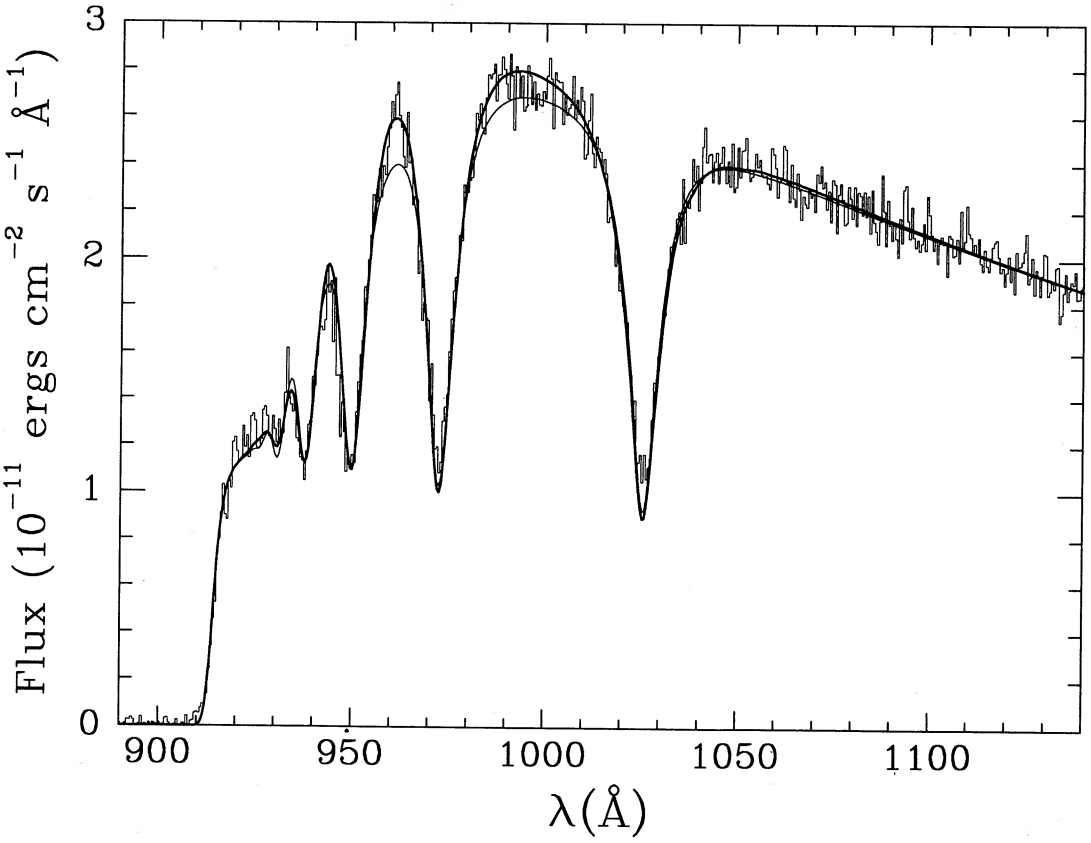

FIG. 4b

FIG. 4.—(*a*) Adopted flux spectrum of G191-B2B. The smooth curve is the Bergeron model calculation ($T_{\rm eff}$ = 59,250 K, log g = 7.5, V = 11.78) with attenuation by interstellar hydrogen with $N_{\rm H} = 1.7 \times 10^{18}$ cm^{-2} and b = 10 km s^{-1} (Kimble et al. 1992). (*b*) Expanded view of sub-Lyman-α spectrum of G191-B2B. The heavy solid line is the Bergeron model, while the light line is from a calculation for the same $T_{\rm eff}$ and log g provided by D. Koester. Both of the models have been smoothed to match the HUT resolution.

area data for the full instrument (the diamonds plotted in Fig. 3, omitting the two suspect points) are also well fitted by a smooth curve. The product of these two curves yields another smoothly varying function that represents our best estimate for the in-flight efficiency of HUT, based purely on our laboratory calibration, and traceable to standards maintained by the National Institute of Standards and Technology. This laboratory calibration curve matches the G191-B2B–based in-flight calibration curve *almost exactly*.

The ratio of the laboratory calibration curve to the in-flight curve has a mean value of 1.003 with an rms deviation of 6.6%, and maximum deviations of +12% and −8%. We emphasize that no rescaling has been done to achieve this impressive agreement. These results provide powerful confirmation that (1) there are no significant systematic errors in the HUT flux calibration, and (2) the G191-B2B model atmosphere calculations provide an excellent flux standard for the far-ultraviolet. We believe our observation of G191-B2B constitutes the best existing absolute UV flux measurement (i.e., directly traceable to laboratory standards) of a star that is suitable as a primary flux standard throughout the vacuum ultraviolet region of the spectrum, all the way to the Lyman limit.

4. SUMMARY

The Hopkins Ultraviolet Telescope performed successfully aboard the Astro-1 Space Shuttle mission and obtained a large number of spectra bearing on a wide range of astrophysical topics in its brief 9 day flight. Observations of the DA white dwarf G191-B2B have been used to derive a photometric calibration curve for HUT that is believed accurate to better than ±10%. The data obtained by HUT represent the first extensive spectrophotometric observations in the 912–1216 Å band to bridge the gap between the Copernicus spectroscopy of bright stars at high resolution, and the *Voyager* observations at much lower resolution. It is expected that improvements to the Shuttle Spacelab systems, especially the IPS performance, together with a longer duration flight and a moderate improvement of the spectrograph efficiency, may enable HUT to obtain nearly an order-of-magnitude more data on the Astro-2 mission, now planned for launch in 1994.

It is a pleasure to acknowledge the assistance of the staff at the Johns Hopkins Applied Physics Laboratory in the design and development of HUT. These include K. Heffernan, B. Ballard, J. Hayes, L. Kohlenstein, and many others. We also thank H. Weaver and K. Chambers for their substantial contributions to the HUT instrument development. E. Mackey (Spacom), R. Crabbs (RSI), and the late V. Muffaletto also contributed significantly to the hardware development. We are grateful to all the NASA personnel who supported the Astro-1 mission, especially J. Jones and T. Gull and the crew of STS-35. One of us (A. F. D.) would particularly like to record his debt to Professor William G. Fastie, who provided invaluable inspiration for this project at its inception.

The Hopkins Ultraviolet Telescope project is supported by NASA contract number NAS5-27000 to the Johns Hopkins University.

REFERENCES

Ballard, B. W. 1984, J. FORTH Appl. Res., 4, 33
Blair, W. P., et al. 1991, ApJ, 379, L33
Boggess, A., et al. 1978, Nature, 275, 372
Broadfoot, A. L., et al. 1977, Space Sci. Rev., 21, 183
Brune, W. H., Mount, G. H., & Feldman, P. D. 1979, ApJ, 227, 884
Carruthers, G. R., Heckathorn, H. M., & Opal, C. B. 1981, ApJ, 243, 855
Cook, T. A., Cash, W., & Snow, T. P. 1989, ApJ, 347, L81
Davidsen, A. F., Fastie, W. G., Feldman, P. D., Hartig, G. F., & Fountain, G. H. 1981, (Proc. SPIE, 265) Shuttle Pointing of Electro-Optical Experiments, 375
Davidsen, A. F., Fastie, W. G., Feldman, P. D., Henry, R. C., & Moos, H. W. 1978, Proposal to NASA, unpublished
Davidsen, A. F., & Fountain, G. H. 1985, Johns Hopkins APL Tech. Dig., 6, 28
Davidsen, A. F., Kimble, R. A., Durrance, S. T., Bowers, C. W. & Long, K. S. 1991a, in Extreme Ultraviolet Astronomy, ed. R. Malina & S. Bowyer (New York: Pergamon), 427
Davidsen, A. F., et al. 1991b, Nature, 351, 128
Feldman, P. D., et al. 1991, ApJ, 379, L37
Ferguson, H. C., et al. 1991, ApJ, 382, L69
Holberg, J. B. in Observatories in Earth Orbit and Beyond, ed. Y. Kondo (Dordrecht: Kluwer), 49
———. 1991, in Extreme Ultraviolet Astronomy, ed. R. Malina & S. Bowyer (New York: Pergamon), 8
Holberg, J. B., Ali, B., Carone, T. E., & Polidan, R. S. 1991, ApJ, 375, 716
Kimble, R. A., et al. 1992, in preparation
Kriss, G. A., et al. 1992, ApJ, in press
Long, K. S., Bowers, C. W., Tennyson, P. P., & Davidsen, A. F. 1985, Adv. Electron. Electron Phys., 64A, 239
Long, K. S., et al. 1991, ApJ, 381, L25
Moos, H. W., et al. 1991, ApJ, 382, L105
Rogerson, J. B., et al. 1973, ApJ, 181, L97
Sciama, D. W. 1990, ApJ, 364, 549
———. 1991, ApJ, 367, L39
Spitzer, L., & Jenkins, D. B. 1975, ARA&A, 13, 133
Woods, T. N., Feldman, P. D., & Bruner, G. H. 1985, ApJ, 292, 676